

Electrochemical Corrosion Behaviour of Pb-free SAC 105 and SAC 305 Solder Alloys: A Comparative Study (Perilaku Kakisan Elektrokimia Aloi Pateri Pb-free SAC 105 dan SAC 305: Suatu Kajian Perbandingan)

M. FAYEKA, A.S.M.A. HASEEB & M.A. FAZAL*

ABSTRACT

Sn-Ag based solder alloy seems to be a promising lead-free solder for the application on electronic assembly. The corrosion behavior of different lead free solder alloys such as Sn-3.0Ag, Sn-1.0Ag-0.5Cu and Sn-3.0Ag-0.5Cu was investigated in 3.5% NaCl solution by potentiodynamic polarization and electrochemical impedance spectroscopy. Scanning electron microscopy (SEM), energy dispersive X-ray spectroscopy (EDX) and X-ray diffraction (XRD) were used to characterize the samples after the tests. The results showed that the addition of 0.5 wt. % copper with Sn-3.0 Ag solder alloy led to a better corrosion resistance while lowering of Ag content from 3.0 to 1.0 wt. % decreased the resistance. Sn-3.0Ag-0.5Cu exhibits a better corrosion resistance in terms of increased charge transfer resistance and impedance values as well as the lowest capacitance. These characteristics signify its suitability for the application in electronic packaging.

Keywords: Corrosion; EIS; Pb-free solders; potentiodynamic polarization

ABSTRAK

Aloi pateri berasaskan Sn-Ag berpotensi menjadi pateri bebas-Pb untuk diaplikasikan sebagai pemasangan elektronik. Tindak balas kakisan aloi pateri bebas Pb yang berbeza seperti Sn-3.0Ag, Sn-1.0Ag-0.5Cu dan Sn-3.0Ag-0.5Cu dikaji dalam larutan 3.5% NaCl menggunakan upaya dinamik pengutuban dan spektroskopi impedans elektrokimia. Mikroskop imbasan elektron (SEM), spektroskopi sinar-X tenaga terserak (EDX) dan pembelauan sinar-X (XRD) telah digunakan untuk mencirikan sampel selepas ujian. Hasil kajian menunjukkan bahawa penambahan 0.5 % bt tembaga ke dalam aloi pateri Sn-3.0Ag menghasilkan rintangan kakisan yang lebih baik. Manakala mengurangkan kandungan Ag daripada 3.0 kepada 1.0 % bt, menurunkan rintangan. Sn-3.0Ag-0.5Cu menunjukkan kakisan yang lebih baik daripada segi peningkatan pemindahan cas rintangan dan nilai impedansi. Ia juga mempunyai kapasitans yang paling rendah. Ciri-ciri ini mencerminkan kesesuaian bahan ini dalam aplikasi pembungkusan elektronik.

Kata kunci: EIS; kakisan; pateri bebas Pb; upaya dinamik pengutuban

INTRODUCTION

Lead-based solders have been widely used in electronic packaging due to their low cost, good wettability, good solderability, low melting temperature and satisfactory mechanical properties (Mohanty & Lin 2006). In spite of having these properties, recently increased environmental and human health concerns over the toxicity of lead and lead-containing compounds have banned the use of Sn-Pb solder alloys (Li et al. 2012). This has promoted the development of new lead free solder alloys to meet its increased demand in modern technology (Fawzy et al. 2014). The potential lead free solders should ensure the melting temperature similar to that of Sn-Pb solders combined with low cost, good solderability, adequate mechanical strength and good corrosion resistance (Billah et al. 2014).

Among the lead-free alloy systems, Sn-Ag is found as one of the earliest commercially available alternative solders (El-Daly et al. 2015). Though Sn-Ag solder exhibits better mechanical properties, the melting temperature is not as low as Sn-Pb solders which necessitates the addition

of other alloying elements to form ternary or higher order solder alloys. For lowering the melting temperature and improving mechanical and wetting properties, attempts have been made by systematic addition of elements as third or higher order (Mohanty & Lin 2013; Rosalbino et al. 2008).

Currently, the ternary eutectic Sn-Ag-Cu (SAC) solder alloys seem to be the most promising candidate for replacement of Pb-containing solders (El-Daly & Hammad 2010). The addition of Cu slightly depresses the melting temperature of Sn-Ag and increases the wetting behavior (Kim et al. 2003). Rosalbino et al. (2009) investigated the corrosion behavior of Sn-Pb, Sn-Ag-In and Sn-Ag-Bi alloys and reported poor corrosion behavior of Sn-Ag-In and Sn-Ag-Bi alloys as compared to that of Sn-Pb. Although additions of Bi and In depressed the melting temperature of Sn-Ag-based lead-free solder alloys (Yeh 2003) and Bi into Sn-Ag system solder improves the wetting/spreading behavior of the solder (Wu et al. 2000), they cannot be a good choice of solder alloy to be used in corrosive environment. Again,

corrosion resistance of the solder strongly depends on its microstructural characteristics. Osorio et al. (2011) reported the results of an electrochemical corrosion study of Sn-Ag solder alloy in 0.5 M NaCl solution. In this study, better corrosion resistance was exhibited for fine dendritic arrays and a mixture of spheroids and fiber-like Ag_3Sn particles. According to (Wang et al. 2012), poor corrosion resistance was exhibited by slowly (furnace cooled) cooled SAC 305 solder due to large Ag_3Sn particles. Therefore, concentration of different alloying element can also play an important role in improving both corrosion resistance properties. Studies on the effect of Cu and Ag on the corrosion behavior of Sn-Ag based solder alloy are scarce. Rosalbino et al. (2009, 2008) investigated corrosion behavior of Sn-3Ag-xCu alloys in 0.1M NaCl solution and compared to that of Sn-Pb solder. The results showed enhanced corrosion resistance with the increase of Cu content. In fact, Sn-Ag-Cu alloys have recently attracted considerable attention and have been proposed by the Japanese (Sn-3Ag-0.5Cu), the European Union (Sn-3.7Ag-0.7Cu) and the United States (Sn-3.9Ag-0.6Cu) consortia to replace Sn-Pb eutectic solder (Mohanty & Lin 2007a). However, there is no in depth study to investigate and compare the corrosion resistance of SAC 105 and SAC 305 solder alloys. The present study aimed to characterize the corrosion behavior of SAC 105 and SAC 305 solder alloys and compare with Sn-3Ag by electrochemical impedance spectroscopy and polarization measurements.

EXPERIMENTAL DETAILS

SAMPLE PREPARATION

The coupons of $\text{Sn}_{97.0}\text{Ag}_{3.0}$, $\text{Sn}_{96.5}\text{Ag}_{3.0}\text{Cu}_{0.5}$ and $\text{Sn}_{98.5}\text{Ag}_{1.0}\text{Cu}_{0.5}$ were cut from the respective solder alloy bar by CNC (Computer Numeric Controlled) lathe machine with a dimension of $1 \times 1 \times 0.8$ cm. Then the coupons were mounted in cold molds using epoxy resins leaving an exposed surface area of 1 cm^2 . A thread was cut over the sample to attach with working electrode holder. Then the specimens were ground using SiC papers of different grits (e.g. 600, 1000, 1200, 1500 and 2000) and fine polished using velvet cloth with Al_2O_3 particle of 6, 1 and $0.2 \mu\text{m}$.

ELECTROCHEMICAL MEASUREMENTS

The electrochemical corrosion of different lead-free solder alloys was investigated in 3.5% NaCl solution. A Gamry Potentiostat (Gamry Instruments, Inc., USA) was used to measure potentiodynamic polarization and impedance spectra. The experiments were carried out in a single compartment cell using a standard three electrode configuration of saturated KCl Ag/AgCl electrode as a reference electrode, platinum wire as a counter electrode and the sample as a working electrode.

Electrochemical impedance spectroscopy measurements were performed at open circuit potential

using 10 mV amplitude sinusoidal signal with 5 points per decade over frequencies ranging from 100 kHz to 100 mHz. The results were area normalized using the Gamry Echem analyst software. Potentiodynamic polarization tests were carried out immediately after the EIS measurements with a potential range of -1000 to +1000 mV versus the reference electrode at a scan rate of 1 mV/s and the sample period was 0.5 mV. Corrosion potential and current density values were determined by Tafel extrapolation method using Echem analyst.

The test methods followed in the present study have similarity with the tests conducted by (Asaduzzaman et al. 2011; Mohanty & Lin 2013; Nazeri & Mohammad 2016; Witte et al. 2006). Duplicate tests were performed under identical testing conditions to verify reproducibility. Note that, potentials reported in this work were all on the Ag/AgCl (in saturated KCl electrolyte) scale.

RESULTS AND DISCUSSION

POTENTIODYNAMIC POLARIZATION RESULTS

Figure 1 shows the potentiodynamic polarization curves for SA, SAC 105 and SAC 305 solder alloys, polarized up to +1000 mV in aerated 3.5% NaCl solution. The corresponding polarization parameters such as corrosion potential (E_{corr}), corrosion current (i_{corr}), passivation potential (E_{pass}) and passivation current (i_{pass}) values obtained from the polarization curves are listed in Table 1. In the following section, a detailed analysis is carried out at different points (A-G) of the polarization curves. The corrosion parameters were determined by Tafel fit using Gamry Echem Analyst DC105 software. It is seen that the critical current density for SAC 105 is comparatively higher than that of other solders.

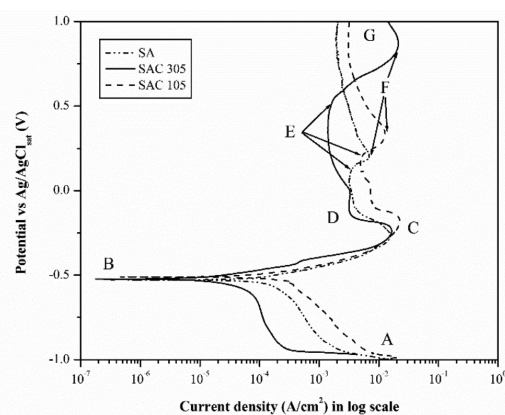
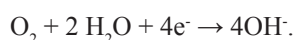


FIGURE 1. Potentiodynamic polarization curves of SA, SAC 305 and SAC 105 solder alloys in 3.5% NaCl solution

Region AB in Figure 1 corresponds to the cathodic reduction reaction. As all the corrosion tests were performed in naturally aerated NaCl solution (neutral solution in terms of pH), the reduction reaction occurring

could be ascribed to the dissolved oxygen reduction reaction (Rosalbino et al. 2008):



The potential at point B is referred to as the corrosion potential (E_{corr}), where the extrapolated anodic and cathodic Tafel slopes intersect and the current becomes zero (Mohanty & Lin 2007). From Table 1, it is seen that the SA solder alloy exhibits a corrosion potential of -528 mV/Ag/AgCl_{sat} which changes to -524 mV/Ag/AgCl_{sat} with the addition of 0.5 wt. % Cu. SAC 105 exhibits the highest E_{corr} value which could be attributed to the decrease of Ag content. The corrosion current density, i_{corr} , is the highest for SA alloy and with the addition of 0.5 wt. % Cu to SA, the i_{corr} value becomes the lowest. When the percentage of Ag is decreased from 3 to 1 wt. % with the same Cu percentage (SAC 105), the corrosion current density becomes higher than that of SAC 305. This demonstrates that SAC 105 is less resistant to corrosion than SAC 305.

On scanning in the anodic direction from point B (Figure 1), the current density rapidly increased due to active dissolution of Sn (Mohanty & Lin 2013). As the electrode potential of both Ag (0.799 V) and Cu (0.337 V) are higher than that of Sn (-0.136 V), Sn works as an anode resulting in its dissolution. Therefore it is assumed that the Sn takes the priority in dissolution to Sn²⁺ and then Sn⁴⁺ according to the following reactions (Mohran et al. 2009):



It has been reported (Hirokazu et al. 2001) that Sn-3.5Ag, Sn-0.8Cu alloy and Sn exhibit the same dissolution characteristics. It is also reported that Sn dissolves faster than other elements in these solder alloys. Additionally, the presence of Ag₃Sn phase in the solders being nobler than Sn accelerates the dissolution of Sn due to galvanic corrosion (Rosalbino et al. 2008). This active dissolution of Sn continues with an increase to a maximum current density up to point C until the hydroxide or oxide concentration reaches to this maximum value (Mohanty & Lin 2013). According to Mohanty and Lin (2007a), solid oxide precipitates on the electrode surface when the solubility product of the tin oxide is exceeded at the anode surface. This phenomenon suggests the formation of a passive film through a dissolution precipitation

mechanism. The current density and the potential at this point are referred to as the critical current density, i_{cc} and passivation potential, E_{pass} , respectively (Rosalbino et al. 2008). From Table 1, SAC 305 exhibits lower i_{cc} value than that of SAC 105.

On further scanning from point C, the current density decreases gradually up to point D indicating formation of passive layer and then at the current density remained independent and almost constant to potential up to point E, which is in good agreement with the findings reported by other researches (Mohanty & Lin 2005; Rosalbino et al. 2009). At point D, the current density is referred to as the passivation current density i_{pass} and the potential range where the current density remains almost constant is the passivation range. Larger passivation range and lower passivation current density indicates more stable and a protective passive film on the surface (Freitas et al. 2014; Osório et al. 2010). From the polarization curves in Figure 1 and Table 1, the passivation range and passivation current density values can be observed for the alloys. The i_{pass} value for Sn-3Ag is decreased with Cu addition in SAC 305 and SAC 105 results in higher i_{pass} . For the passivation range, Sn-3Ag has ΔE value of 193.33mV that increased to 557.96mV for SAC 305. For SAC 105, ΔE is lower than that of SAC 305. So, the SAC 305 exhibits the largest passivation range and the lowest passivation current density indicating its highest corrosion resistance. Larger passivation range is attributed to higher Ag content in presence of Cu in the solder alloy, which is in a good agreement with other researchers (Rosalbino et al. 2009).

Beyond point E, a rapid increase in the current density occurs at high potential, polarizing up to point F, which is referred to as the transpassive potential or breakdown potential (Liu et al. 2015). This increment in current density is due to the breakdown of the passive oxide layer at high potential. The breakdown of the passive film can also be caused by the presence of Cl⁻ on the surface (Liu et al. 2015; Mohanty & Lin 2005). Scanning more from point F results in a decrease in the current density. This decrease is due to the formation of corrosion product that covers the whole surface of the solder preventing further corrosion.

Figure 2 shows the SEM/EDX results of the solder alloys at as-received condition and after polarization up to critical current density (point C in Figure 1). The appearance of all the as-received solder surface are almost similar (Figure 2(a)-2(c)). The as-received SAC solders consist of primary β -Sn phase and intermetallic compounds including Ag₃Sn and Cu₆Sn₅ (Rosalbino et al. 2009).

TABLE 1. Potentiodynamic polarization parameters for SA, SAC 305 and SAC 105 solder alloys in 3.5% NaCl solution

| Solder | E_{corr} (mV) | i_{corr} (mA/cm ²) | E_{pass} (mV) | i_{cc} (mA/cm ²) | i_{pass} (mA/cm ²) | ΔE (mV) |
|---------|------------------------|---|------------------------|---------------------------------------|---|-----------------|
| SA | -528 | 3.85 | -271 | 15.76 | 4.13 | 193.33 |
| SAC 305 | -524 | 27.8×10^{-3} | -234 | 16.38 | 3.16 | 538.78 |
| SAC 105 | -510 | 318×10^{-3} | -189 | 22.55 | 7.74 | 234.87 |

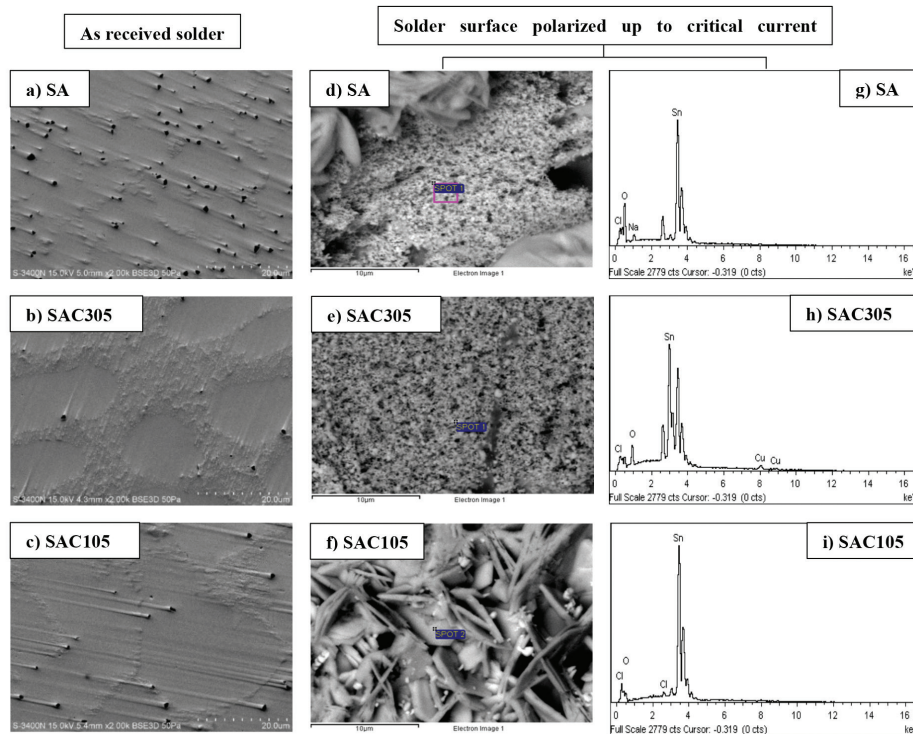


FIGURE 2. SEM micrographs at as-received condition (a-c), surface products after polarization up to critical current density (d-f) and EDX spectrum after polarization up to critical current density (g-i) of SA, SAC 305 and SAC 105 solder alloys, respectively

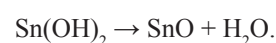
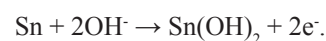
After polarization up to critical current density, different solder alloys show degradation of the surface at different level. It is believed that due to corrosion at critical current density, the surface gets supersaturated with oxides and different corrosion compounds (Mohanty & Lin 2013). Corrosion rate could be high due to dissolution of these compounds partially or completely in solution. From the EDX results, it is seen that the presence of oxygen in SAC 105 (Figure 2(i)) is less than both SA and SAC 305. So the corrosion product of SAC 105 is not so adherent to the surface. In case of SAC 305 in Figure 2(h), presence of Cu in the corrosion product can be noticed which could contribute to the formation of any intermetallic compound which makes the product more adherent to the surface. Some pits are observed in SA and SAC 105 alloy surface that could be caused by electrochemical reaction of the β -Sn phase with Cl^- ions indicating less corrosion resistance of these alloys (Rosalbino et al. 2008). The corrosion product of SAC 305 exhibits a fine fibrous structure while SAC 105 exhibits fiber and plate like structure. SA exhibits a mixture of both fine fibrous and plate like structure over the surface. The presence of Cl^- in the region FG (Figure 1) is also confirmed from EDX analysis and SEM micrograph of the corroded specimen after the end of electrochemical experiment shown in Figure 3. The SEM micrographs of the solder surface showed that the surface was completely covered with corrosion products suggesting higher Ag content resulted in better corrosion resistance. The EDX results shown in Figure 3 suggest that the corrosion products contain Sn, Cl and O indicating

possible formation of tin oxychlorides. Gao et al. (2012) have reported that the corroded product $\text{Sn}_3\text{O}(\text{OH})_2\text{Cl}_2$ exhibits both needle-like and plate-like products, which can also be observed in Figure 3.

From the micrographs shown in Figure 3, it can be observed that SAC 105 and SAC 305 shows platelet-like shape with a size difference. The corrosion product on the SAC 305 solder surface was observed to be more compact and adherent thus providing better corrosion resistance.

Figure 4 shows the XRD patterns for SAC 105 and SAC 305 solder alloys after the electrochemical corrosion tests. Several phases are detected at the exposed surface which are $\text{Sn}_3\text{O}(\text{OH})_2\text{Cl}_2$, $\text{Sn}_3\text{O}_2(\text{OH})_2$, SnO_2 , SnO , Cu_6Sn_5 and Ag_3Sn . This result is in accordance with that obtained from EDX analysis. No peak of pure Sn is detected which indicates that the surface is fully covered with corrosion products where $\text{Sn}_3\text{O}(\text{OH})_2\text{Cl}_2$ could be the dominant one.

The formation of oxides of tin may take place through the following reactions (Mohran et al. 2009).



Further oxidation of SnO leads to formation of stannic hydroxide which may partially hydrate to stannic oxide as shown in the following reaction (Nazeri & Mohamad 2014):



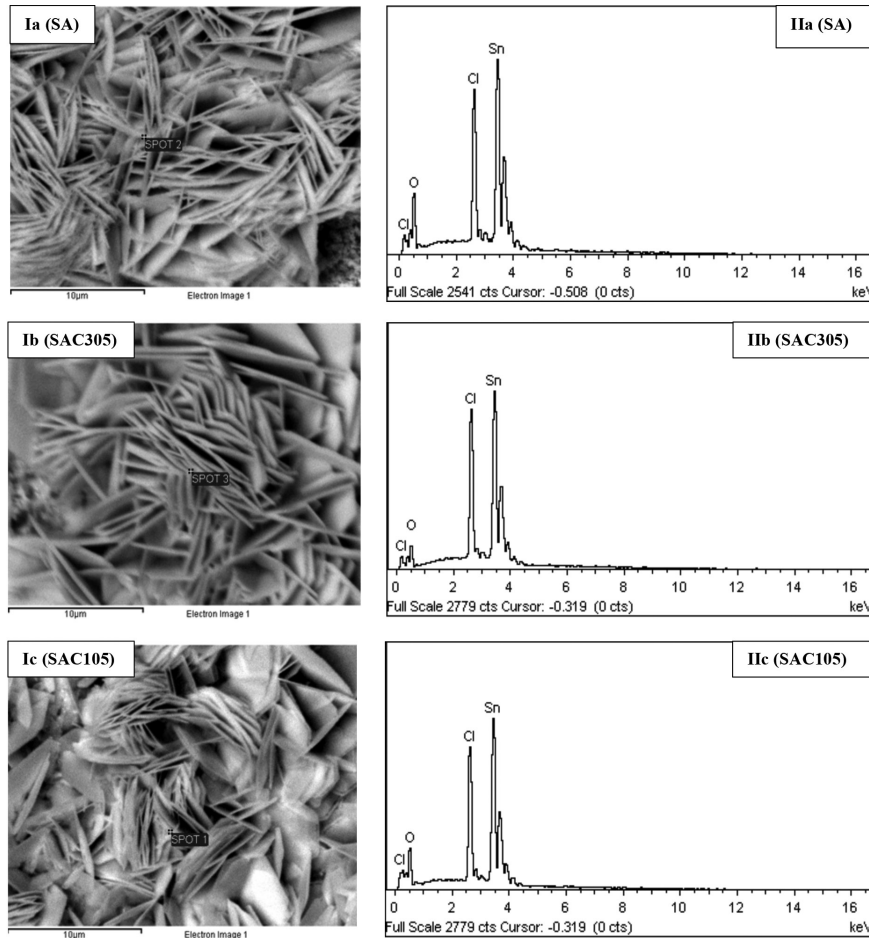
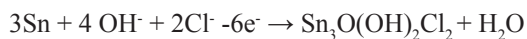


FIGURE 3. SE micrographs (I) of the corrosion products and EDX spectrum (II) of solder alloys (a) SA, (b) SAC 305 and (c) SAC 105 solder alloys, respectively, after the completion of polarization in Figure 1

The product undergoes dehydration as follows:
 $\text{Sn}(\text{OH})_4 \rightarrow \text{SnO} + \text{H}_2\text{O}$.

$\text{Sn}(\text{OH})_4$ is highly insoluble resulting in precipitation giving rise to a more protective passivating film and its stability increases with the dehydration reaction (Abd El Rehim et al. 2006). Therefore, the formation of tin oxides is thermodynamically favored. From the XRD patterns shown in Figure 4, the corroded product on SAC 105 and SAC 305 is confirmed to be $\text{Sn}_3\text{O}(\text{OH})_2\text{Cl}_2$, which is similar to results obtained by other researches (Gao et al. 2012). This might have formed according to the following reaction (Rosalbino et al. 2009):



The formation of the oxides at the sample surface introduces passivation and thereby contributes in reducing corrosion rate.

ELECTROCHEMICAL IMPEDANCE SPECTROSCOPY (EIS)

The impedance spectra of the solder alloys are illustrated in Figures 5 and 6. Nyquist plots are shown in Figure 5 for the solder alloys, where difference in the diameter of

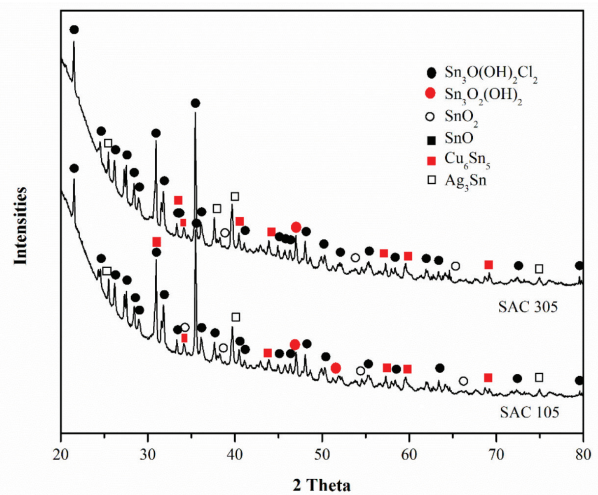


FIGURE 4. X-ray diffraction scans after polarization tests for SAC 305 and SAC 105

the impedance loops for different solder alloys can be observed. Nyquist plots are characterized by a semicircle or capacitive loop from high to low frequencies where these capacitive loops are ascribed to the double layer

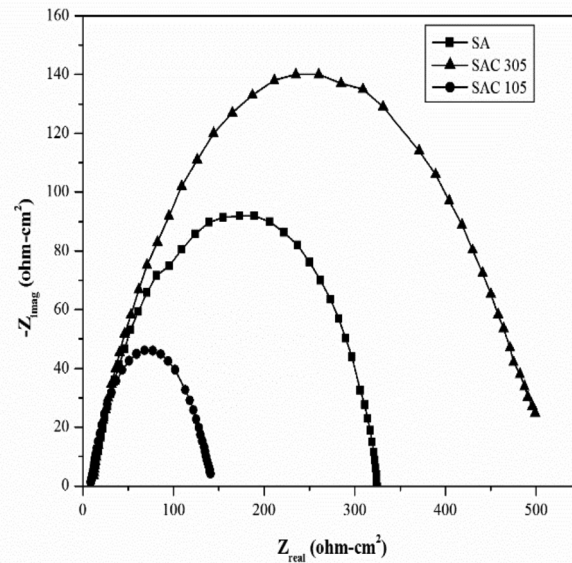


FIGURE 5. Nyquist plot for SA, SAC 305 and SAC 105 solder alloys in 3.5% NaCl solution

capacitance and charge transfer resistance (Okafor et al. 2009). In this study, the obtained curves are approximated by a single capacitive semicircle which is ascribed to the double layer capacitance and charge transfer resistance (Okafor et al. 2009; Raja et al. 2013). Increasing impedance loop diameter has a relation to decreasing corrosion rate. In Figure 5, the loop diameter of the Sn-Ag solder increased with addition of 0.5 wt. % Cu (SAC 305). The loop diameter was drastically decreased for SAC 105. The loop diameter for Sn-1.0Ag-0.5Cu is smaller than that of Sn-3Ag. This demonstrates that certain percentage of Ag (e.g. 3.0 wt. % Ag) is important to increase the corrosion resistance with the addition of Cu. This behavior is consistent with findings by Rosalbino et al. (2008) with the polarization results in Figure 1.

The charge transfer resistance, R_{ct} can be obtained from the semicircle diameter of the Nyquist plot. Capacitance, C_{dl} can be calculated using (1) where the characteristic frequencies f_{max} were obtained from the semicircles maxima (Okafor et al. 2009). The electrochemical parameters are shown in Table 2.

$$C_{dl} = \frac{1}{2\pi f_{max} R_{ct}} \quad (1)$$

It can be seen from Table 2 that SAC 305 alloy exhibits highest resistance and lowest capacitance values among all the three solders. These results reflect the formation of a more adherent and compact corrosion products film at the surface of SAC 305 solder (Brett & Trandafir 2004). The results are consistent with the findings by Rosalbino et al. (2009).

As a consequence, better corrosion resistance shown by SAC 305 alloy with respect to SA and SAC 105 could be ascribed to improved protective properties of the corrosion products layer which acts as an effective barrier against corrosion progress. The Bode plots for different solder

alloys are illustrated in Figure 6. The Bode plot in Figure 6(a) shows the influence of ohmic drop in 3.5% NaCl solution for different solder alloys (Díaz-Ballote et al. 2009). The impedance magnitudes of the three solder alloy samples at lowest frequency have been listed in Table 2. The highest magnitude of impedance is observed for the SAC 305 indicating the highest corrosion resistance. This seems to be attributed to the formation of comparatively more adherent and protective oxide film on the surface.

From the respective phase angle Bode plots in Figure 6(b), the maximum phase angle values are exhibited at high frequency which were attributed to the formation of protective oxide films (Yuan et al. 2007). From Table 2, it can be observed that the largest maximum phase angle, θ_{max} is exhibited by SAC 305 solder alloy which confirms its highest corrosion resistance. It can be seen that SAC 305 solder alloy exhibits highest resistance and lowest capacitance which reflect the formation of a more adherent and compact corrosion product film acting as an effective barrier against further corrosion.

CONCLUSION

Among the lead-free solders used in electronic packaging, Sn-Ag-Cu emerges as the primary choice for replacing lead-solders. Electrochemical corrosion investigation of SAC 105 and SAC 305 was done to compare their corrosion properties. Potentiodynamic polarization tests and electrochemical impedance spectroscopy measurements showed a better corrosion resistance of Sn-3Ag-0.5Cu alloy compared to SAC 105 and SA solder alloys in 3.5% NaCl solution. Addition of Cu with Sn-3.0Ag solder resulted enhanced corrosion resistance. This could be as a result of higher passivation range with lower passivation current density. Characterization performed at the end of electrochemical tests evidenced the presence of a corrosion

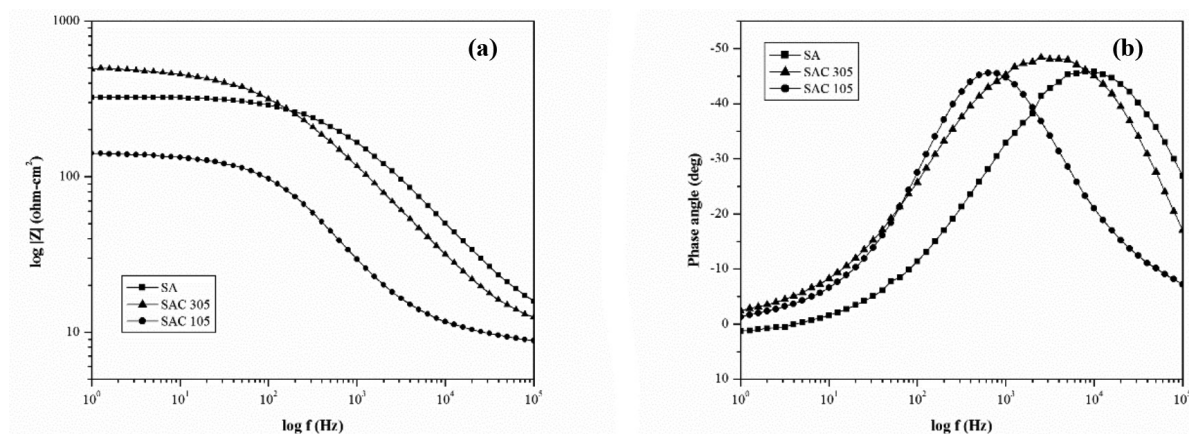


FIGURE 6. Bode plots (a) magnitude bode plot and (b) phase angle bode plot for SA, SAC 305 and SAC 105 solder alloys in 3.5% NaCl solution

TABLE 2. Electrochemical impedance spectroscopy parameters for SA, SAC 305 and SAC 105 solder alloys in 3.5% NaCl solution

| Solder Alloys | R_{ct} (Ω -cm ²) | f_{max} (Hz) | C_{dl} (μ F/cm ²) | $\log Z $ (Ω) | θ_{max} ($^{\circ}$) |
|---------------|--|--------------------|--------------------------------------|-------------------------|-------------------------------|
| SA | 311.03 | 1.59×10^2 | 3.22×10^{-6} | 323.8 | 46.2 |
| SAC 305 | 490.36 | 1.26×10^2 | 2.57×10^{-6} | 490.25 | 48.4 |
| SAC 105 | 136.69 | 2.0×10^2 | 5.82×10^{-6} | 139.35 | 45.6 |

products layer constituted by tin oxyhydroxychloride at the exposed surface which seems to be more adherent and compact for SAC 305. The electrochemical impedance spectroscopy results in highest charge transfer resistance with lowest double layer capacitance and the highest impedance exhibited by SAC 305 indicating better corrosion resistance than SAC 105 and SA solder alloys. Therefore, SAC 305 serves as the best corrosion resistant solder alloy among the studied solder alloys for electronic packaging.

ACKNOWLEDGEMENTS

The authors would like to acknowledge the financial support of UMRG grant (UMRG no. RP013B-13AET) from the University of Malaya, Malaysia.

REFERENCES

- Abd El Rehim, Sayed S, Ayman M Zaky & Noble F Mohamed. 2006. Electrochemical behaviour of a tin electrode in tartaric acid solutions. *Journal of Alloys and Compounds* 424(1): 88-92.
- Asaduzzaman, M.D., Chand Mustafa Mohammad & Islam Mayeedul. 2011. Effects of concentration of sodium chloride solution on the pitting corrosion behavior of AISI 304L austenitic stainless steel. *Chemical Industry and Chemical Engineering Quarterly* 17(4): 477-483.
- Billah, Md Muktedir, Kazi Mohammad Shorowordi & Ahmed Sharif. 2014. Effect of micron size Ni particle addition in Sn-8Zn-3Bi lead-free solder alloy on the microstructure, thermal and mechanical properties. *Journal of Alloys and Compounds* 585(0): 32-39.
- Brett, C.M.A. & Trandafir, F. 2004. The corrosion of dental amalgam in artificial salivas: An electrochemical impedance study. *Journal of Electroanalytical Chemistry* 572(2): 347-354.
- Díaz-Ballote, L., López-Sansores, J.F., Maldonado-López, L. & Garfias-Mesias, L.F. 2009. Corrosion behavior of aluminum exposed to a biodiesel. *Electrochemistry Communications* 11(1): 41-44.
- El-Daly, A.A., El-Taher, A.M. & Gouda, S. 2015. Development of new multicomponent Sn-Ag-Cu-Bi lead-free solders for low-cost commercial electronic assembly. *Journal of Alloys and Compounds* 627(0): 268-275.
- El-Daly, A.A. & Hammad, A.E. 2010. Effects of small addition of Ag and/or Cu on the microstructure and properties of Sn-9Zn lead-free solders. *Materials Science and Engineering: A* 527(20): 5212-5219.
- Fawzy, A., Fayek, S.A., Sobhy, M., Nassr, E., Mousa, M.M. & Saad, G. 2014. Tensile creep characteristics of Sn-3.5 Ag-0.5 Cu (SAC355) solder reinforced with nano-metric ZnO particles. *Materials Science and Engineering: A* 603: 1-10.
- Freitas, E.S., Osório, W.R., Spinelli, J.E. & Garcia, A. 2014. Mechanical and corrosion resistances of a Sn-0.7 wt. % Cu lead-free solder alloy. *Microelectronics Reliability* 54(6): 1392-1400.
- Gao, Y-F., Cheng, C-Q., Zhao, J., Wang, L-H. & Li, X-G. 2012. Electrochemical corrosion of Sn-0.75 Cu solder joints in NaCl solution. *Transactions of Nonferrous Metals Society of China* 22(4): 977-982.
- Kim, K.S., Huh, S.H. & Sukanuma, K. 2003. Effects of intermetallic compounds on properties of Sn-Ag-Cu lead-free soldered joints. *Journal of Alloys and Compounds* 352(1): 226-236.
- Li, X., Zu, F., Gao, W., Cui, X., Wang, L. & Ding, G. 2012. Effects of the melt state on the microstructure of a Sn-3.5%Ag solder

- at different cooling rates. *Applied Surface Science* 258(15): 5677-5682.
- Liu, M., Yang, W., Ma, Y., Tang, C., Tang, H. & Zhan, Y. 2015. The electrochemical corrosion behavior of Pb-free Sn-8.5 Zn-XCr solders in 3.5 wt. % NaCl solution. *Materials Chemistry and Physics* 168: 27-34.
- Mohanty, U.S. & Lin, K-L. 2013. Corrosion behavior of Pb-free Sn-1Ag-0.5Cu-XNi solder alloys in 3.5% NaCl solution. *Journal of Electronic Materials* 42(4): 628-638.
- Mohanty, U.S. & Lin, K-L. 2007a. Electrochemical corrosion study of Sn-XAg-0.5 Cu alloys in 3.5% NaCl solution. *Journal of Materials Research* 22(09): 2573-2581.
- Mohanty, U.S. & Lin, K-L. 2007b. The polarization characteristics of Pb-free Sn-8.5 Zn-XAg-0.1 Al-0.05 Ga alloy in 3.5% NaCl solution. *Corrosion Science* 49(7): 2815-2831.
- Mohanty, U.S. & Lin, K-L. 2006. Effect of Al on the electrochemical corrosion behaviour of Pb free Sn-8.5 Zn-0.5 Ag-XAl-0.5 Ga solder in 3.5% NaCl solution. *Applied Surface Science* 252(16): 5907-5916.
- Mohanty, U.S. & Lin, K-L. 2005. Electrochemical corrosion behaviour of lead-free Sn-8.5 Zn-X Ag-0.1 Al-0.5 Ga solder in 3.5% NaCl solution. *Materials Science and Engineering: A* 406(1): 34-42.
- Mohran, HossniaS, Abdel-Rahman El-Sayed & HanyM Abd El-Lateef. 2009. Anodic behavior of tin, indium, and tin-indium alloys in oxalic acid solution. *Journal of Solid State Electrochemistry* 13(8): 1279-1290.
- Nazeri, Muhammad Firdaus Mohd & Ahmad Azmin Mohamad. 2016. Corrosion resistance of ternary Sn-9Zn-xIn solder joint in alkaline solution. *Journal of Alloys and Compounds* 661: 516-525.
- Nazeri, Muhammad Firdaus Mohd & Ahmad Azmin Mohamad. 2014. Corrosion measurement of Sn-Zn lead-free solders in 6M KOH solution. *Measurement* 47(0): 820-826.
- Okafor, P.C., Liu, X. & Zheng, Y.G. 2009. Corrosion inhibition of mild steel by ethylamino imidazole derivative in CO₂-saturated solution. *Corrosion Science* 51(4): 761-768.
- Osório, W.R., Garcia, L.R., Peixoto, L.C. & Garcia, A. 2011. Electrochemical behavior of a lead-free SnAg solder alloy affected by the microstructure array. *Materials & Design* 32(10): 4763-4772.
- Osório, W.R., Cremasco, A., Andrade, P.N., Garcia, A. & Caram, R. 2010. Electrochemical behavior of centrifuged cast and heat treated Ti-Cu alloys for medical applications. *Electrochimica Acta* 55(3): 759-770.
- Raja, Pandian Bothi, Ahmad Kaleem Qureshi, Afidah Abdul Rahim, Hasnah Osman & Khalijah Awang. 2013. *Neolamarckia cadamba* alkaloids as eco-friendly corrosion inhibitors for mild steel in 1M HCl media. *Corrosion Science* 69: 292-301.
- Rosalbino, F., Angelini, E., Zanicchi, G., Carlini, R. & Marazza, R. 2009. Electrochemical corrosion study of Sn-3Ag-3Cu solder alloy in NaCl solution. *Electrochimica Acta* 54(28): 7231-7235.
- Rosalbino, F., Angelini, E., Zanicchi, G. & Marazza, R. 2008. Corrosion behaviour assessment of lead-free Sn-Ag-M (M= In, Bi, Cu) solder alloys. *Materials Chemistry and Physics* 109(2): 386-391.
- Hirokazu Tanaka, Fumitaka Ueta, Sachio Yoshihara & Takashi Shirakashi. 2001. Effects of reflow processing and flux residue on ionic migration of lead-free solder plating using the quartz crystal microbalance method. *Materials Transactions* 42(9): 2003-2007.
- Wang, M., Wang, J., Feng, H. & Ke, W. 2012. Effect of Ag₃Sn intermetallic compounds on corrosion of Sn-3.0 Ag-0.5 Cu solder under high-temperature and high-humidity condition. *Corrosion Science* 63: 20-28.
- Witte, F., Fischer, J., Nellesen, J., Crostack, H-A., Kaese, V., Pisch, A., Beckmann, F. & Windhagen, H. 2006. *In vitro* and *in vivo* corrosion measurements of magnesium alloys. *Biomaterials* 27(7): 1013-1018.
- Wu, C.M.L., Huang, M.L., Lai, J.K.L. & Chan, Y.C. 2000. Developing a lead-free solder alloy Sn-Bi-Ag-Cu by mechanical alloying. *Journal of Electronic Materials* 29(8): 1015-1020.
- Yeh, M.S. 2003. Effects of indium on the mechanical properties of ternary Sn-In-Ag solders. *Metallurgical and Materials Transactions A* 34(2): 361-365.
- Yuan, S.J., Choong, A.M.F. & Pehkonen, S.O. 2007. The influence of the marine aerobic *Pseudomonas* strain on the corrosion of 70/30 Cu-Ni alloy. *Corrosion Science* 49(12): 4352-4385.

Department of Mechanical Engineering
University of Malaya
50603 Kuala Lumpur, Federal Territory
Malaysia

*Corresponding author; email: fazal@um.edu.my

Received: 17 September 2015

Accepted: 24 May 2016